

Supporting Information

Nanozymes promote electrocatalytic nitrogen oxidation

Zuochao Wang^a, Jiao Liu^a, Huan Zhao^a, Wenxia Xu^a, Jiaxin Liu^a, Ziyi Liu^a, Jianping Lai^{a,*} and Lei Wang^{a,b,*}

^a State Key Laboratory of Eco-chemical Engineering, International Science and Technology Cooperation Base of Eco-chemical Engineering and Green Manufacturing, College of Chemistry and Molecular Engineering, Qingdao University of Science and Technology, Qingdao 266042, P. R. China

^b Shandong Engineering Research Center for Marine Environment Corrosion and Safety Protection, College of Environment and Safety Engineering, Qingdao University of Science and Technology, Qingdao 266042, P. R. China

Correspondence and requests for materials should be addressed to J. L. (e-mail: jplai@qust.edu.cn) and L.W. (e-mail: inorchemwl@126.com)

1. Experimental Procedures

1.1 Ion-concentration detection methods. The electrolytes pre and post test were first diluted to appropriate concentration and then tested using a UV-Vis spectrophotometer to quantify the concentration. The concentrations of nitrate-N, nitrite-N and ammonia-N were estimated by UV-Vis spectrophotometry according to the standard method.¹

1.2 Determination of NO_x. NO_x was determined using N-(1-naphthyl)-ethylenediamine dihydrochloride spectrophotometric method with some modification.² Specifically, 0.4 g of sulfanilic acid was dissolved in 5 mL of H₂O and 1 mL of phosphoric acid. Then add 20 mg of N-(1-naphthyl)-ethylenediamine dihydrochloride and dilute the volume to 100 mL to obtain the chromogenic agent. 1 mL treated electrolyte was mixed with 4 mL chromogenic agent and left in darkness for 30 min, and measure the UV-Vis absorption spectrum at 540 nm. Calibrate the concentration-absorbance curve with a series of standard potassium nitrite solutions in 0.1 M Na₂SO₄ solution.

1.3 Determination of nitrate-N. First, a certain amount of electrolyte was taken out of the electrolytic cell and diluted to 5 mL to the detection range. Then, 0.1 mL 1 M HCl and 0.01 mL 0.8 wt% sulfamic acid solution were added to the aforementioned solution. The absorption spectrum was tested using an ultraviolet-visible spectrophotometer and the absorption intensities at wavelengths of 220 and 275 nm were recorded. The final absorbance value was calculated using the equation: $A = A_{220\text{nm}} - 2A_{275\text{nm}}$.³ The concentration-absorbance curve was made using a series of standard potassium nitrate solutions and the potassium nitrate crystal was dried at 105–110 °C for 2 h in advance.

1.4 Calculation of the Turnover frequency (TOF).

$$\text{TOF} = n/(\text{N} \times t)$$

Where n is the number of moles of product, N is the mole of active metal sites, t is the electrolysis time (10 h).⁴

1.5 ¹⁵N₂ isotope-labeling Experiment

For isotope labeling experiments, we carried out the batch experiments using $^{15}\text{N}_2$ as the feeding gas for five consecutive times and collected all the electrolytes. $^{15}\text{N}_2$ gas was pre-purified through 0.1 M NaOH, 0.05 M H_2SO_4 and Na_2SO_4 . To increase the concentration of $^{15}\text{NO}_3^-$ for isotopic mass spectrometry, the obtained solution was concentrated by 5 times via distilling at 70 °C. For comparison, $^{14}\text{N}_2$ with natural abundance ^{15}N (0.36 atom%) was used as a feeding gas with other conditions being consistent. Notably, the pre-purging time for isotope labeling experiment was only 5 min owing to the high price of $^{15}\text{N}_2$ gas.

2. Electrochemical characterization.

Typically, 3 mg of electrocatalyst and 10 μL of 5 wt.% Nafion solution were dispersed in 1 mL of ethanol by sonicating for 1 h to form a homogenous ink. Then the as-prepared ink was loaded onto a carbon paper within an area of $1\times 1\text{ cm}^2$ and dried under vacuum condition overnight. All electrochemical NOR tests were carried out at room temperature in a gas-tight two compartment H-type cell, which was separated by a Nafion 117 membrane (DuPont). Note that Nafion membrane is impermeable to anions. Before the tests, the Nafion membrane was pre-treated in 3% H_2O_2 solution and 5% H_2SO_4 solution as well as ultra-pure (UP) water in sequence. The high-purity N_2 (99.9995%) and Ar (99.9995%) gas were prepurified by passage through an acidic solution and a silica gel sorbent tube to remove any possible sources of N contamination (e.g. ammonia), and subsequently bubbled through the electrolyte for at least half hour before NOR tests. Cleaning of the $^{15}\text{N}_2$ gas (98 atom% ^{15}N , Sigma-Aldrich) is very important, because $^{15}\text{N}_2$ may contain substantial impurities in the form of $^{15}\text{NH}_3$ along with $^{15}\text{NO}_x$ species. We tested the purity of our $^{15}\text{N}_2$ by first saturating our solution of 0.1 M KOH with Ar to remove any excess $^{14}\text{N}_2$, followed by bubbling around 200 ml of $^{15}\text{N}_2$. We circulated the 200 ml $^{15}\text{N}_2$ gas for 1 h to duplicate the long-term electrochemical measurement. To remove these impurities, a Cu impurity trap was introduced, composed of 2 g Cu-Zn-Al oxide catalyst in a U-shaped stainless steel tubing. The Cu catalyst was reduced before each experiment in a 5% H_2/Ar stream at 300 °C for 2 h. The gas flow was switched to Ar at 300 °C for 30 min, and the Cu

impurity trap was cooled to $-100\text{ }^{\circ}\text{C}$ using an ethanol slurry, prepared by mixing ethanol with liquid nitrogen. Ar flow through the Cu impurity trap was used to purge the entire system for 30 min, including the gas-tight electrochemical cell. The electrolyte was then injected using a syringe to the Ar-purged electrochemical cell to prevent exposure to air and moisture. Ar was bubbled through the electrolyte for an additional 30 min to remove dissolved $^{14}\text{N}_2$. Finally, $^{15}\text{N}_2$ was introduced to the electrochemical system through the reduced Cu impurity trap. After bubbling $^{15}\text{N}_2$ gas for 15 min (about 200 ml), the gas was circulated in a closed loop using a glass pump (Makuhari Rikagaku Garasu). Using this cleaning procedure, three repeated measurements were carried out. All the gases were purified by the Cu impurity trap. Before the electrolysis, the Ar was plunged into the electrolyte about 1 h, then $^{15}\text{N}_2$ was plunged into the electrolyte to saturation. The procedure that detected $^{14}\text{NO}_3^-$ produced was the same except the $^{14}\text{N}_2$ (99.999%) was used. Linear sweep voltammogram (LSV) was performed in a 0.1 M Na_2SO_4 solution at a scan rate of 5 mV s^{-1} . For NOR experiments, potentiostatic tests were conducted in the N_2 -saturated 0.1 M Na_2SO_4 electrolyte with continuous N_2 feeding. Furthermore, the concentration of produced nitrate was systematically detected and quantified by ion chromatography (930 compact IC Flex, Metrohm). Additionally, for $^{15}\text{N}_2$ isotope (Sigma-Aldrich, 98 atom % ^{15}N) labelling experiment, after 50 h of NOR with $^{15}\text{N}_2$ feeding gas, the obtained $^{15}\text{NO}_3^-$ containing electrolyte was analyzed by ^{15}N nuclear magnetic resonance (NMR, JEOL ECA400). D_2O was applied as the solvent and the reaction time of each NMR test was 11 hours with 11000 scans. Note that the test electrolytes were subjected to the concentration treatment (to 0.5 mL) before both IC and NMR analysis.

The yield rate of nitrate production was calculated by the following equation:⁵

$$r=(C\times V)/(t\times m)$$

where C is the measured nitrate molar concentration, V is the volume of the electrolyte, t is the electrochemical oxidation reaction time, and m is the loading mass of the electrocatalysts.

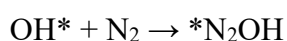
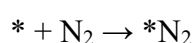
The Faradaic efficiency of nitrate formation can be calculated as follow:

$$FE=(5F\times C\times V)/Q$$

where F is the Faraday constant, C is the measured nitrate concentration, V is the volume of the electrolyte, and Q is the total charge passed through the electrode in the electrocatalytic process.

3. Density functional theory (DFT) calculations.

In Density Functional Theory calculations, we built slab model of Co_3O_4 (311). The vacuum layer along z direction was set to be 15\AA to avoid the interactions between images. Structural optimization calculation were performed by Vienna Ab-initio Simulation Package (VASP) with the projector augmented wave (PAW) method. The exchange-functional was treated using the Perdew-Burke-Ernzerhof (PBE) functional, in combination with the DFT-D3 correction. The cut-off energy of the plane-wave basis is set at 450 eV. For the optimization of both geometry and lattice size, the Brillouin zone integration is performed with $2\times 2\times 1$ Gamma k-point sampling. The self-consistent calculations applied a convergence energy threshold of 10^{-5} eV. The equilibrium geometries and lattice constants were optimized with maximum stress on each atom within 0.01 eV/\AA . In Gibbs free energy calculation, we built the hydrogen adsorption model by employing the computational hydrogen electrode (CHE) model developed by Nørskov et al. The elementary steps of N_2 activation are described as follows:



Gibbs free energy of OH were obtained at pH=13. Gibbs free energy of intermediates were calculated as $G = E + E_{\text{zpe}} - TS$, where E, E_{zpe} and S indicate energy, zero-point energy and entropy of surface adsorbing H atom, respectively. Besides, the Kelvin temperature T was set to be 298.15 K.

4. Supplementary Figures

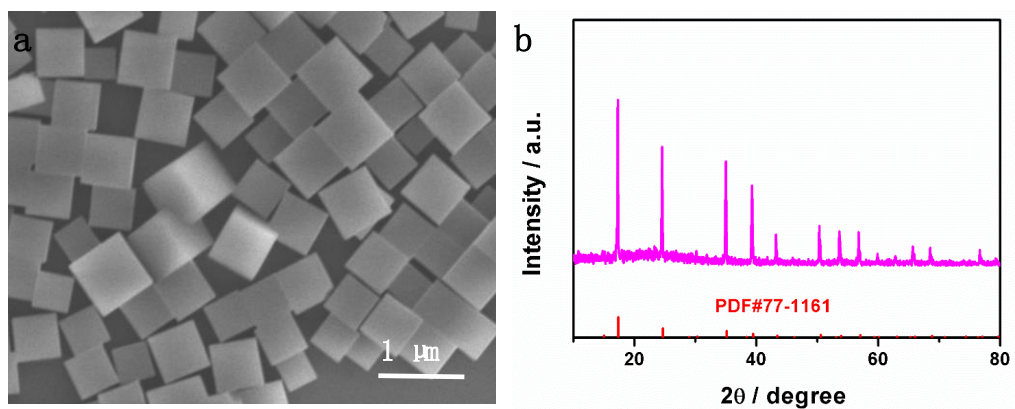


Fig. S1. (a) SEM image and (b) XRD pattern of PBA.

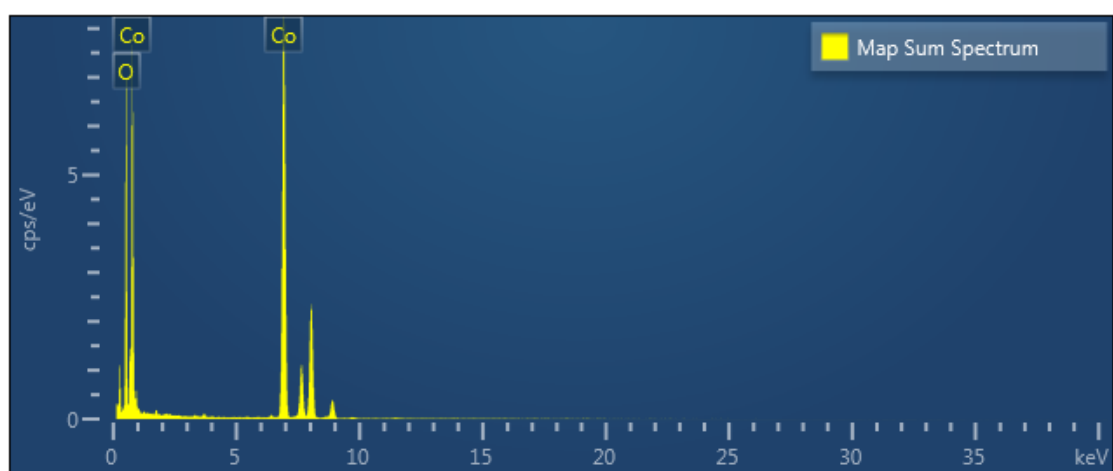


Fig. S2. TEM EDX pattern of Co_3O_4 NBs.

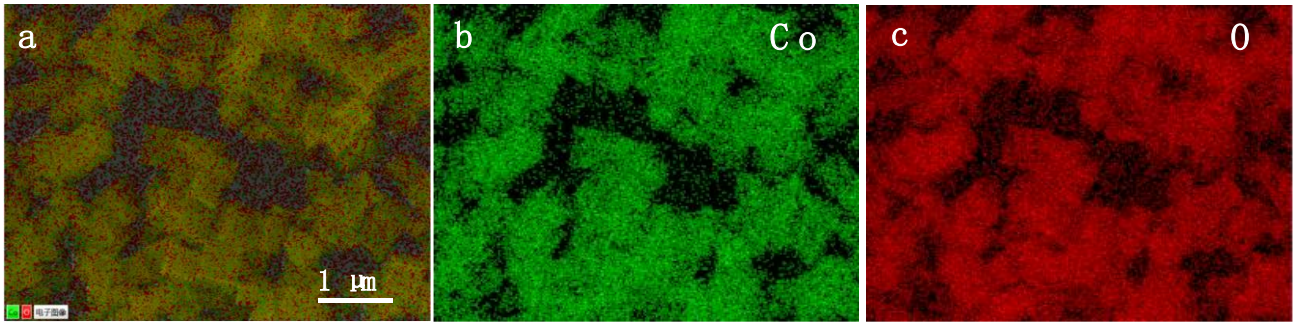


Fig. S3. SEM EDX mapping image of Co_3O_4 NBs.

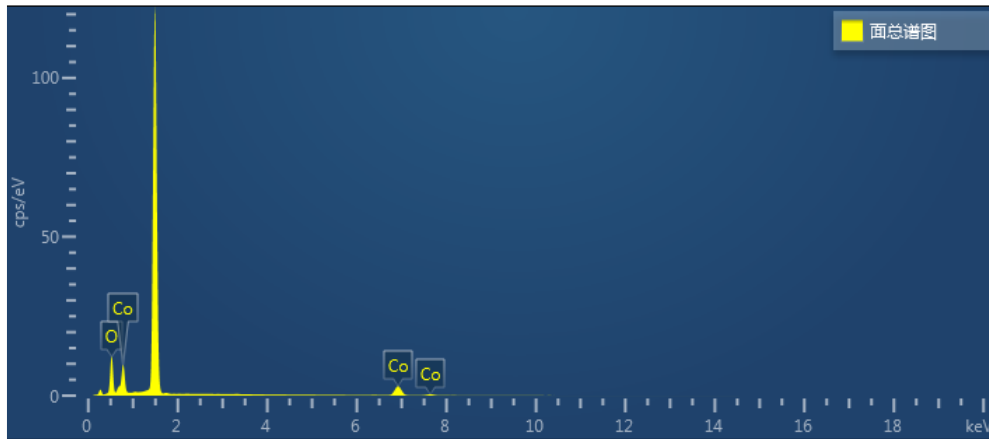


Fig. S4. SEM EDX pattern of Co_3O_4 NBs.

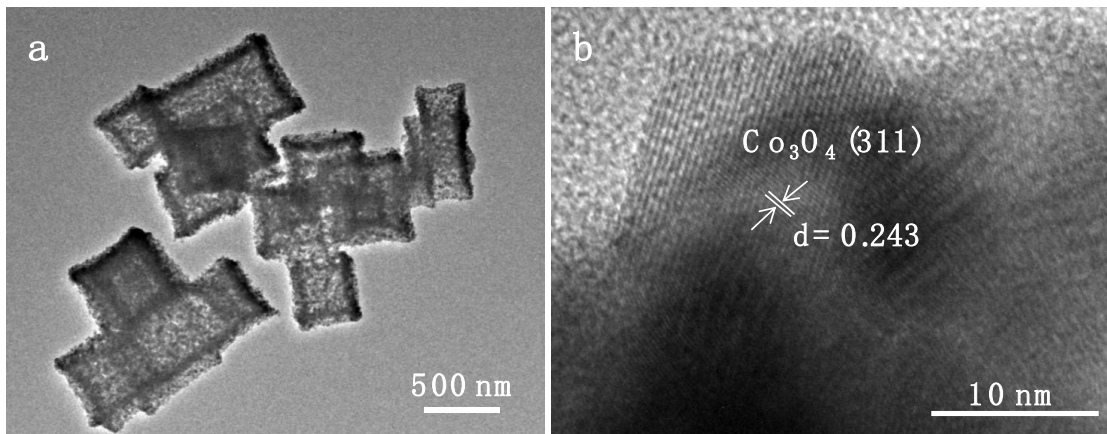


Fig. S5. (a) TEM and HRTRM images of Co_3O_4 NBs.

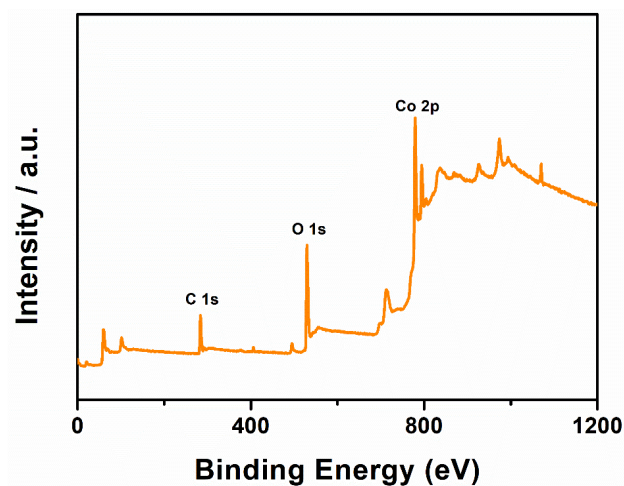


Fig. S6. XPS surveyspectra of Co₃O₄ NBs.

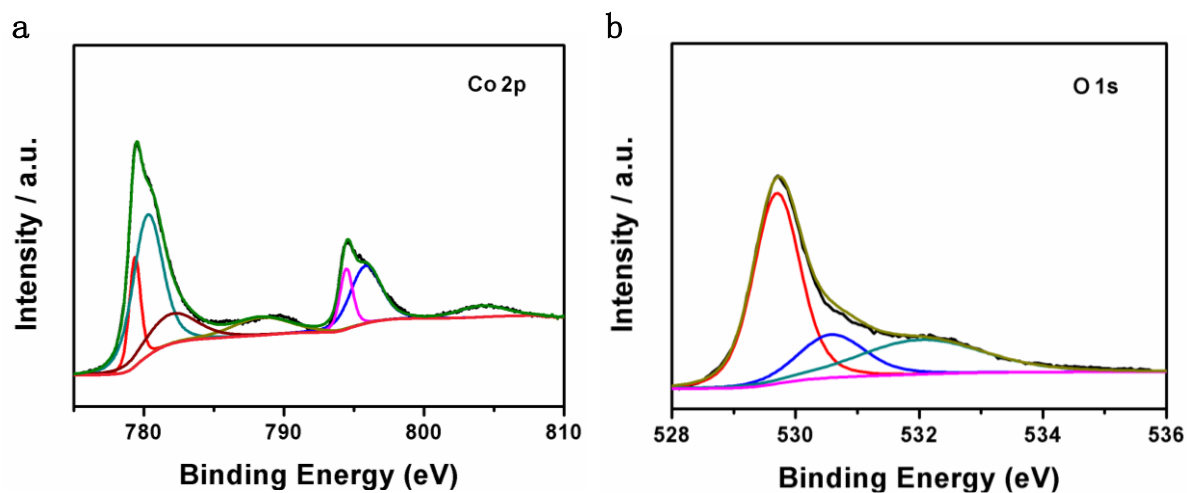


Fig. S7. XPS spectra of (a) Co 2p and (b) O 1s signals in Co₃O₄ NBs.

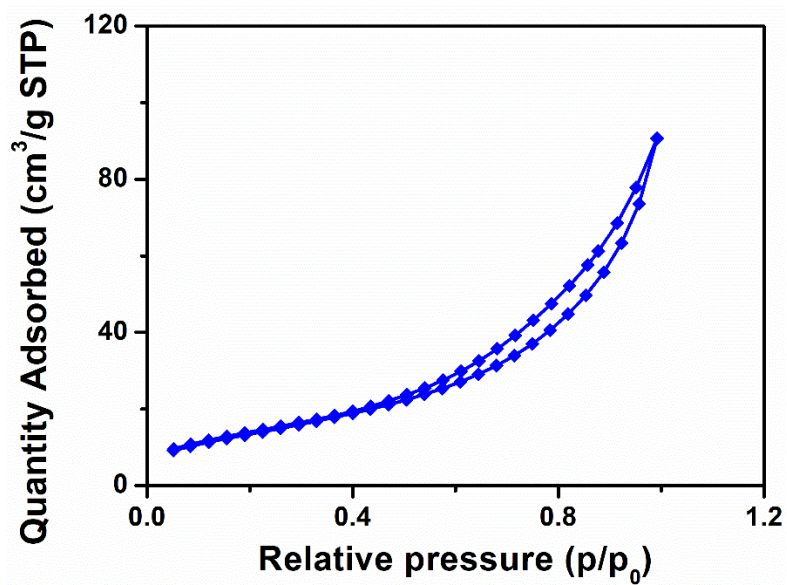


Fig. S8. N_2 adsorption and desorption isotherms of Co_3O_4 NBs.

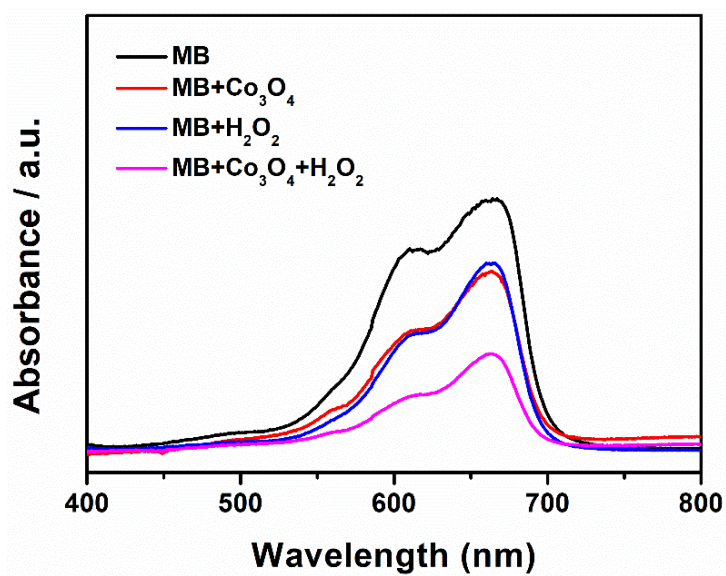


Fig. S9. Absorption spectra probing the formation of $\bullet OH$ through the reaction of $\bullet OH$, and color deletion of methylene blue, MB.



Fig. S10. Photograph of catalyst yield after increasing the amount of reactants.

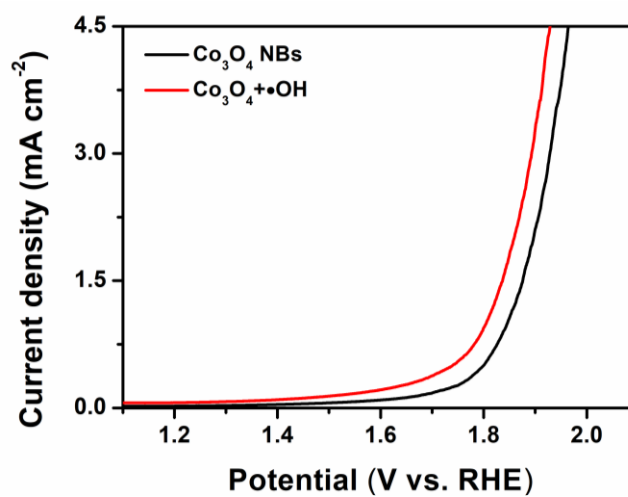


Fig. S11. LSV curves of Co₃O₄+•OH and Co₃O₄ NBs in N₂-saturated 0.1 M Na₂SO₄ with a scan rate of 5 mV s⁻¹.

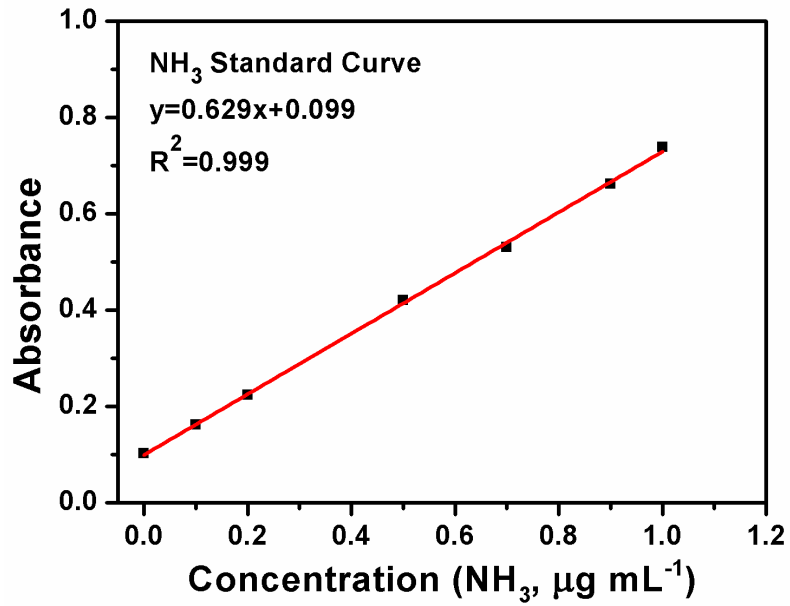


Fig. S12. The calibration curves for the colorimetric NH_3 assay using the indophenol blue method in 0.1 M Na_2SO_4 .

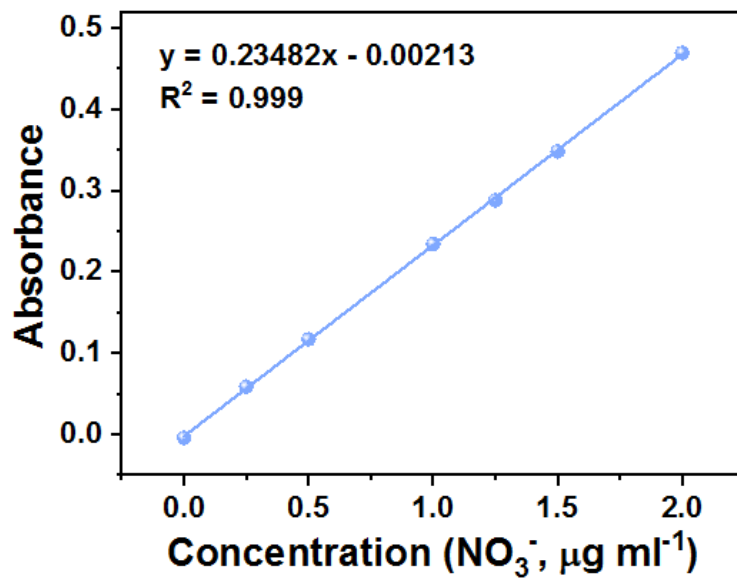


Fig. S13. The UV-Vis absorption spectra and the corresponding standard curves NO_3^- in 0.1 M Na_2SO_4 as background solution.

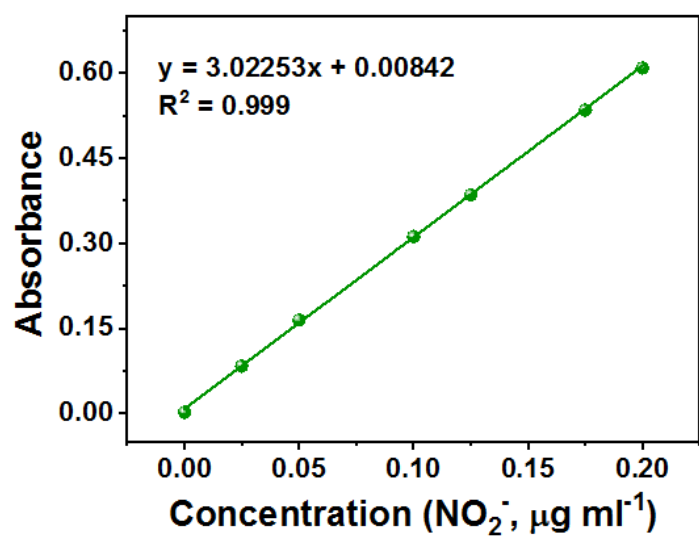


Fig. S14. The UV-Vis absorption spectra and the corresponding standard curves NO_2^- in 0.1 M Na_2SO_4 as background solution.

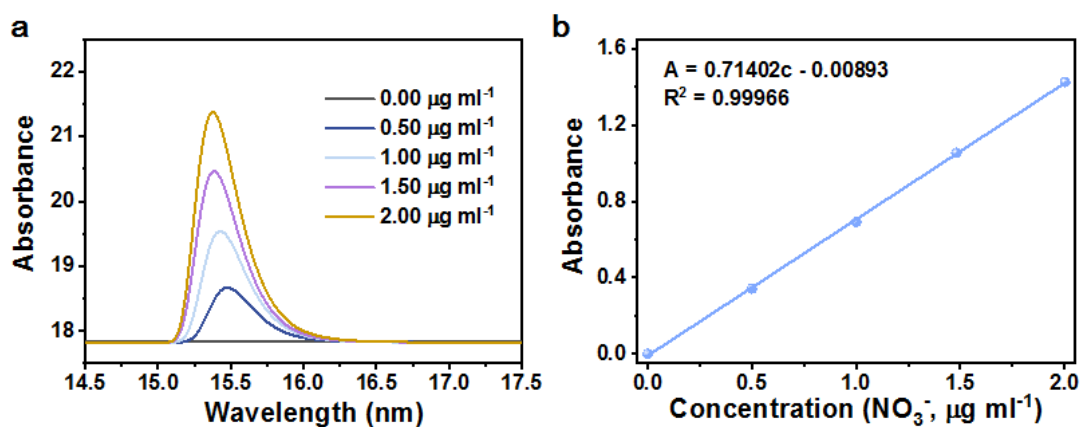


Fig. S15. (a) Ion chromatogram curves of a series of standard nitrate solution; (b) calibration curve of IC for nitrate concentration.

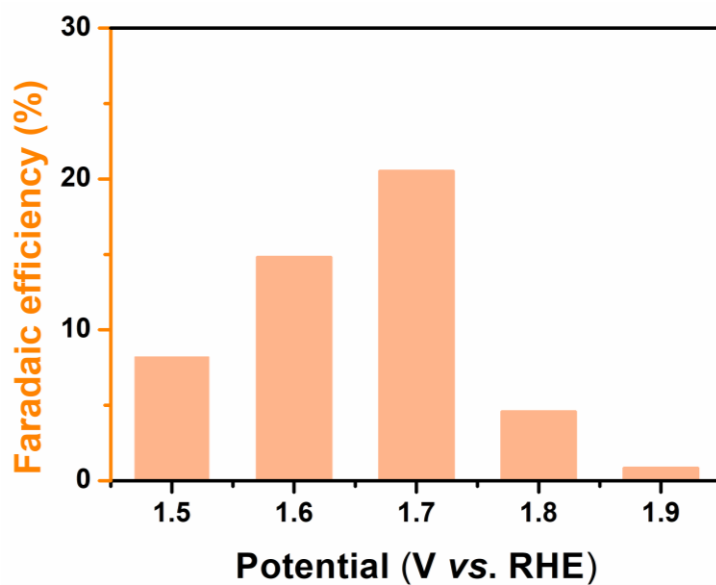


Fig. S16. FEs of $\text{Co}_3\text{O}_4+\bullet\text{OH}$ at various potential in N_2 -saturated 0.1 M Na_2SO_4 electrolytes.

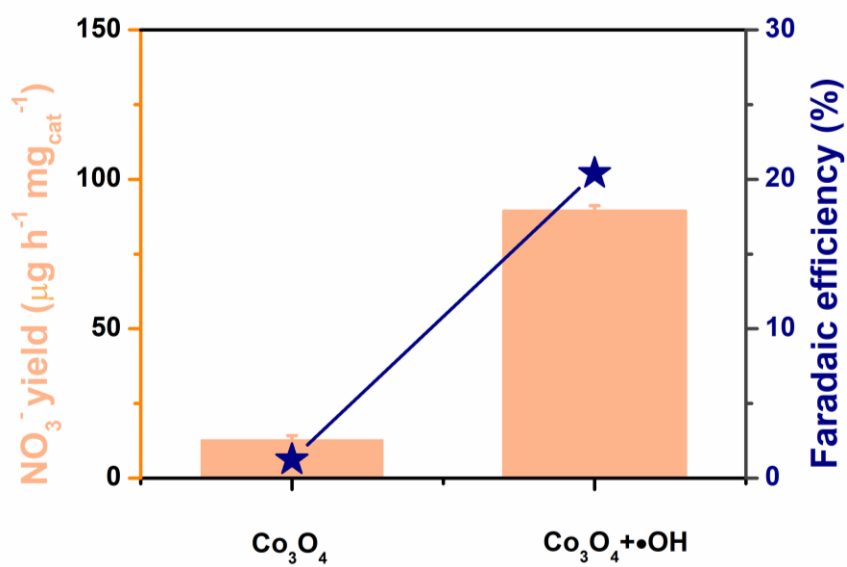


Fig. S17. NO_3^- yield rate and FEs of $\text{Co}_3\text{O}_4+\bullet\text{OH}$ and Co_3O_4 NBs at 1.7 V vs. RHE.

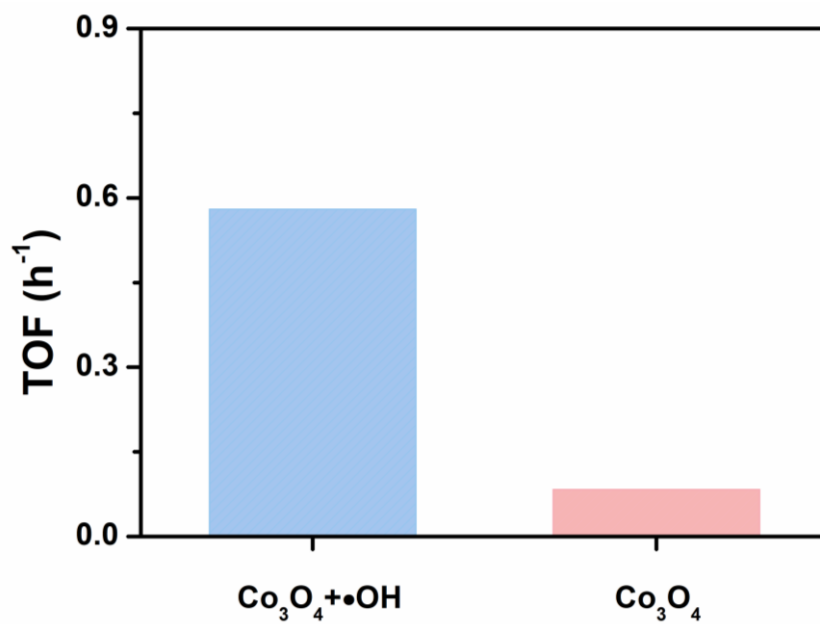


Fig. S18. The TOF values of $\text{Co}_3\text{O}_4+\bullet\text{OH}$ and Co_3O_4 NBs at 1.7 V vs. RHE.

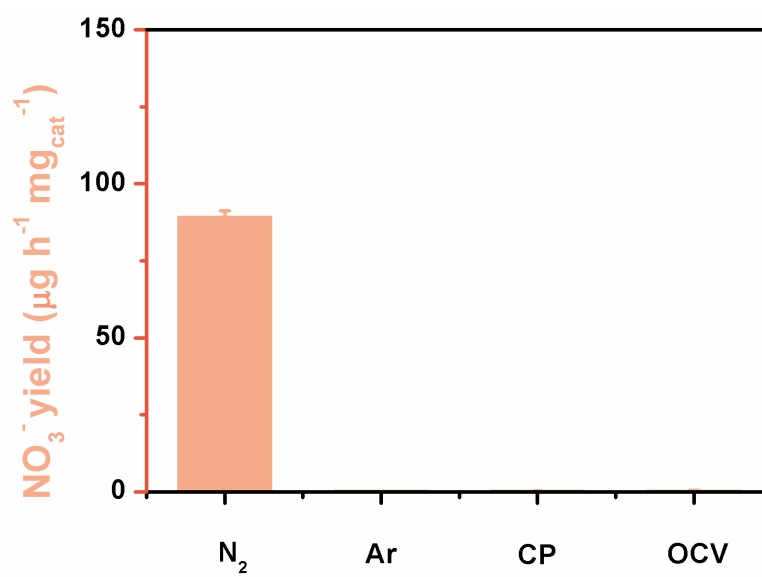


Fig. S19. The yield of NO_3^- under different conditions.

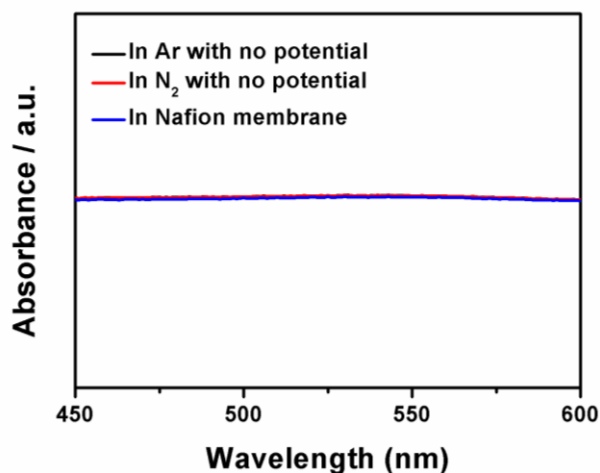


Fig. S20. UV-vis absorption spectra of the electrolyte at different conditions (Black line for continuous Ar bubbling experiments with no potential applied without nanozymes; red line for continuous N₂ bubbling experiments with no potential applied without nanozymes; blue line for Nafion membrane in the cell, respectively.).

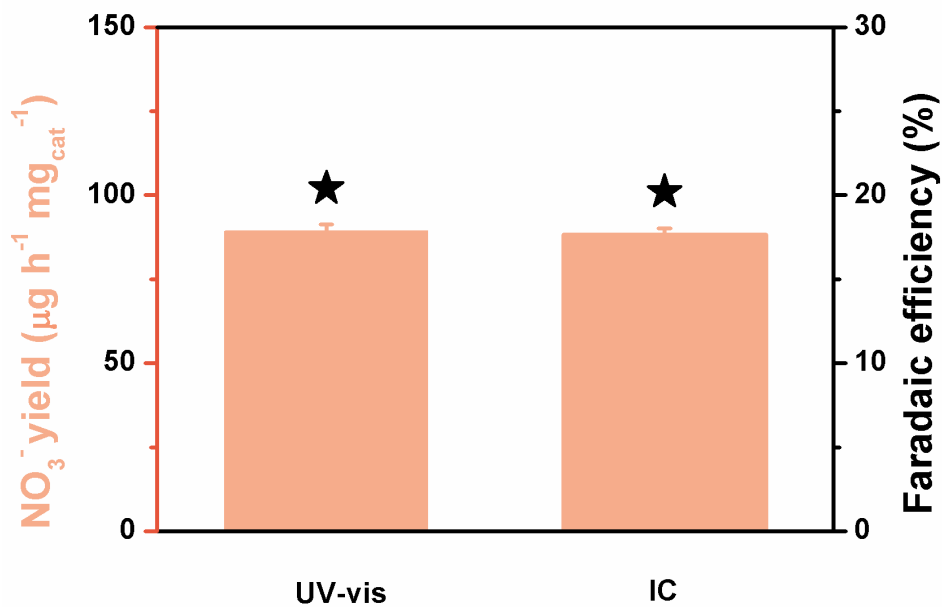


Fig. S21. Ion chromatography method and the colorimetric method for NO₃⁻ yield of nanozymes in N₂-saturated 0.1 M Na₂SO₄ electrolyte after 10 h electrolysis at 1.7 V vs. RHE.

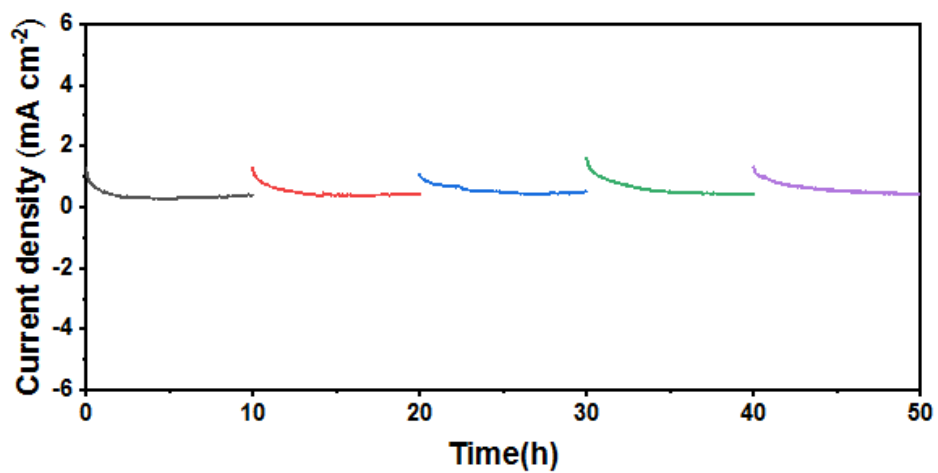


Fig. S22. Time-dependent current density curves of nanozymes with 10 h for each cycle in N₂-saturated 0.1 M Na₂SO₄ solution.

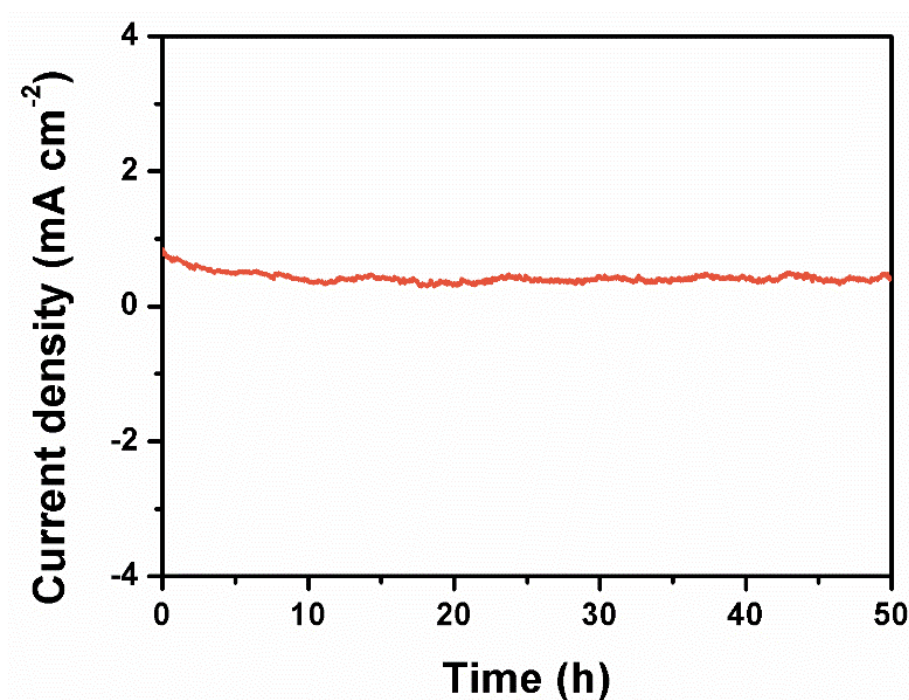


Fig. S23. Long-time chronoamperometry curve of nanozymes at 1.7 V vs. RHE.

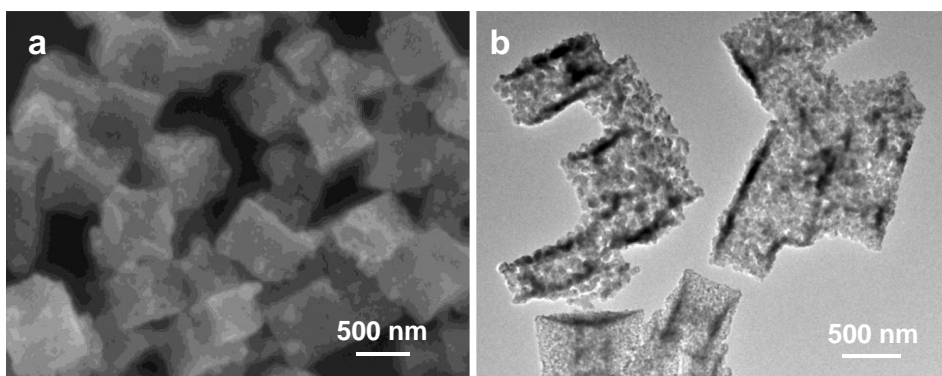


Fig. S24 (a) SEM and (b) TEM images of the catalyst after stability test.

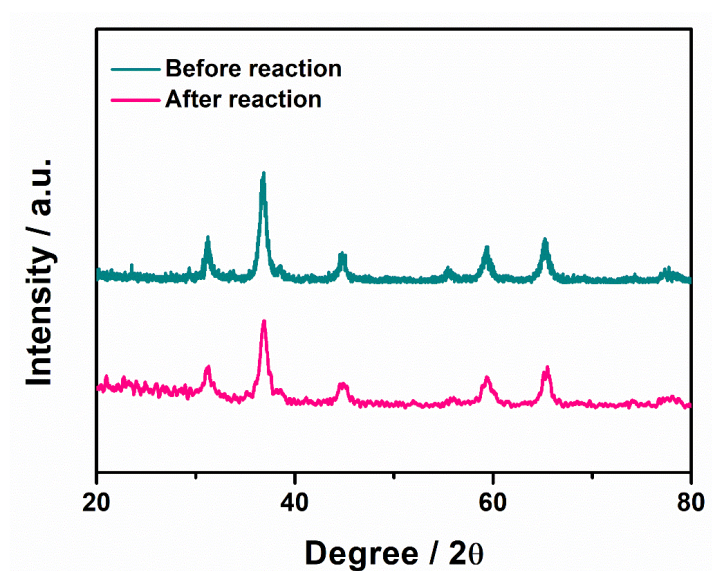


Fig. S25. XRD pattern of the catalyst after stability test.

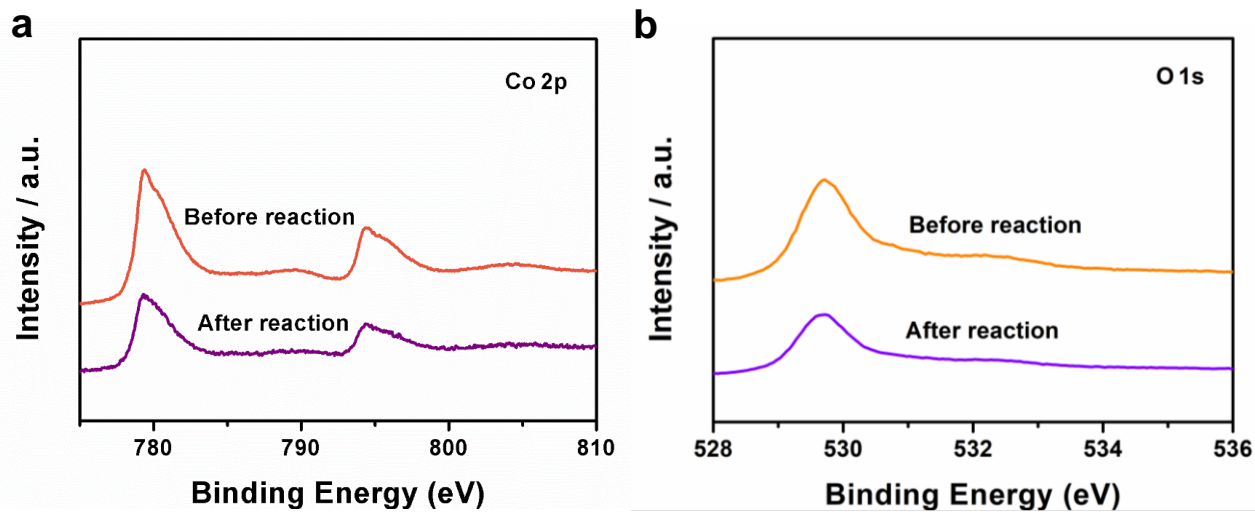


Fig. S26. XPS spectra of Co_3O_4 NBs: Co 2p (a) and O 1s (b) after stability test.

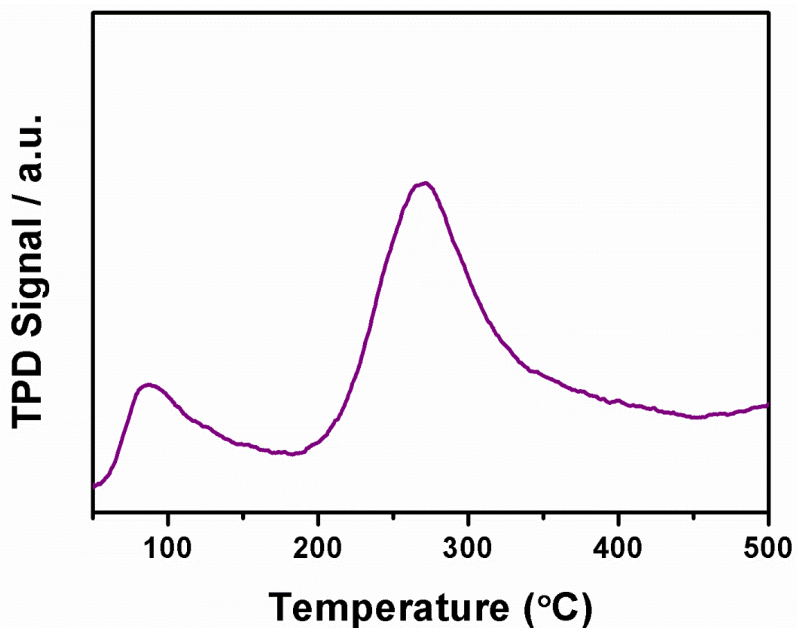


Fig. S27. N_2 -TPD of Co_3O_4 NBs.

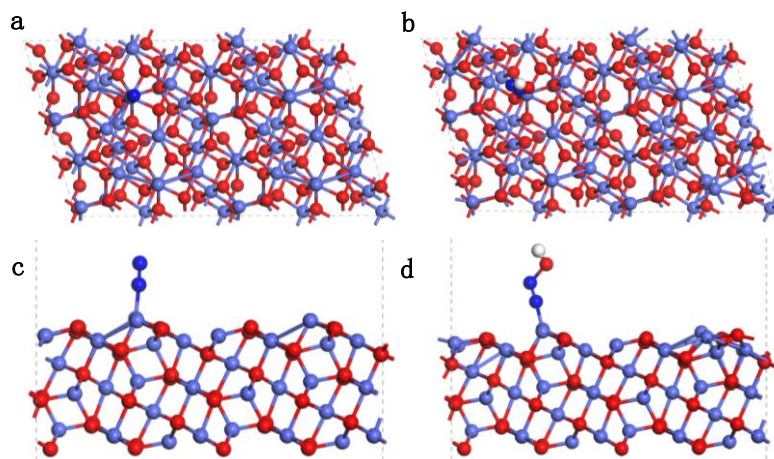


Fig. S28. Top (a) and side (b) view of Co_3O_4 absorbing N_2 . Top (b) and side (d) view of Co_3O_4 absorbing N_2OH . Co, O and N atoms are indicated by blue, red and navy balls, respectively.

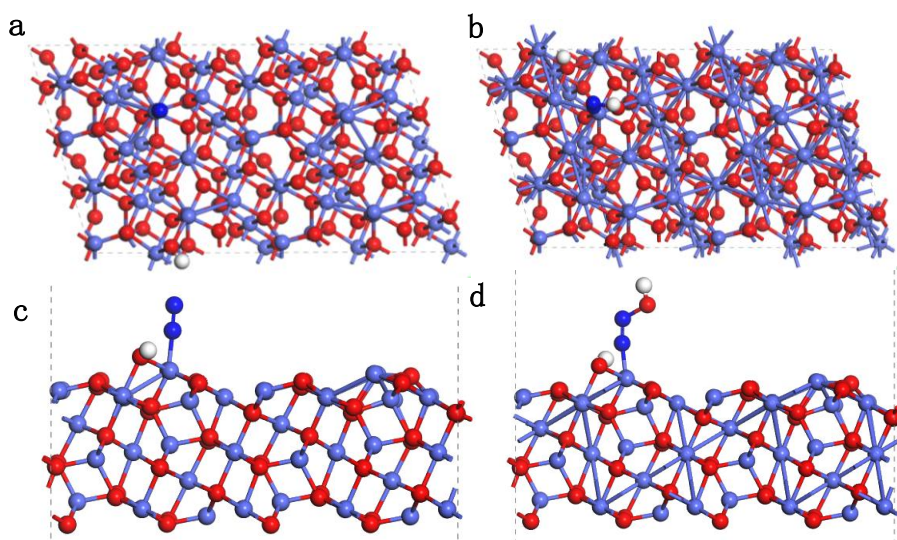


Fig. S29. Top (a) and side (b) view of Co_3O_4 absorbing N_2 and OH. Top (b) and side (d) view of Co_3O_4 absorbing N_2OH and OH. Co, O and N atoms are indicated by blue, red and navy balls, respectively.

5. Supplementary Tables

Table S1. Comparison of the NOR performance of nanozyme with other non-noble catalysts reported to date under ambient conditions (room temperature and atmospheric pressure).

Catalyst	Electrolyte	NO ₃ ⁻ Yield	FE (%)	References
Nanozyme	0.1 M Na ₂ SO ₄	89.35 μg mg ⁻¹ _{cat} h ⁻¹ (1.7 V)	20.4 (1.7 V)	This work
Co ₃ O ₄ NBs	0.1 M Na ₂ SO ₄	12.8 μg mg ⁻¹ _{cat} h ⁻¹ (1.7 V)	1.23 (1.7 V)	This work
Mn ₃ O ₄	0.1 M Na ₂ SO ₄	4.3 μg mg ⁻¹ _{cat} h ⁻¹ (1.7 V)	7.6 (1.7 V)	6

6. References

1. T. Li, S. Han, C. Wang, Y. Huang, Y. Wang, Y. Yu and B. Zhang, *ACS Catal.*, 2021, **11**, 14032-14037.
2. N. Zhang, L. Li, J. Wang, Z. Hu, Q. Shao, X. Xiao and X. Huang, *Angew. Chem. Int. Ed.*, 2020, **59**, 8066-8071.
3. C. W. Shuhe Han, Yuting Wang, Yifu Yu, Bin Zhang, *Angew. Chem. Int. Ed.*, 2021, **60**, 4474-4478.
4. P. Gao, Z.-H. Xue, S.-N. Zhang, D. Xu, G.-Y. Zhai, Q.-Y. Li, J.-S. Chen and X.-H. Li, *Angew. Chem. Int. Ed.*, 2021, **60**, 20711-20716.
5. T. Li, S. Han, C. Cheng, Y. Wang, X. Du, Y. Yu and B. Zhang, *Angew. Chem. Int. Ed.*, 2022, **61**, e202204541.
6. Z. Nie, L. Zhang, X. Ding, M. Cong, F. Xu, L. Ma, M. Guo, M. Li and L. Zhang, *Adv. Mater.*, 2022, **34**, 2108180.